

# Relationship between soil CO<sub>2</sub> flux and tectonic structures in SW Sicily

Marco Camarda<sup>1</sup>, Sofia De Gregorio<sup>\*,1</sup>, Roberto M.R. Di Martino<sup>1</sup>, Rocco Favara<sup>1</sup>, Vincenzo Prano<sup>1</sup>

<sup>(1)</sup> Istituto Nazionale di Geofisica e Vulcanologia, sezione di Palermo – Via Ugo La Malfa, 153 - 90146 Palermo, Italy

Article history: received July 1, 2019; accepted January 15, 2020

## Abstract

The identification and characterization of seismogenic structures in southwestern Sicily is an open debate both for the geological-structural complexity of this sector and the scarce seismicity as well. In addition, clear morphological evidence of tectonic structures is limited. Besides the geophysical methods, the study of the spatial distribution of soil CO<sub>2</sub> flux is a valid methodology to investigate the position and geometry of buried active faults. Indeed, active tectonic structures are channels with high permeability through which deep fluids can migrate toward the atmosphere. Therefore, the alignment of high degassing areas can reveal the presence of preferential ways of rising fluids (i.e. faults). We applied this methodology in SW Sicily in the surrounding of the area hit by the 1968 seismic sequence and in three other areas where evidence of active deformation has been recognized. Furthermore, to investigate the origin of emitted fluids, we measured the carbon isotopic composition of the soil CO<sub>2</sub> in some high emission sites. The results showed high spatial variability of soil CO<sub>2</sub> fluxes with values ranging from 1 to 430 g m<sup>-2</sup>d<sup>-1</sup>. The areal patterns of soil CO<sub>2</sub> fluxes in all the areas reveal a strong influence of the main tectonic structures and active deformations on soil CO<sub>2</sub> emissions. The range of isotopic data and the distribution of soil CO<sub>2</sub> fluxes suggest a supply of deep fluids through the active tectonic structures.

Keywords: Soil CO<sub>2</sub> flux; Diffusive degassing structures (DDS); Active tectonic structures; Belice Valley.

---

## 1. Introduction

In southwestern Sicily, only sporadic and low magnitude earthquakes have been usually recorded. A striking exception to this feature is represented by the seismic sequence occurred from January 14 – 25, 1968, in Belice Valley area, with eight major events of magnitude between 4.7 and 5.4 [Anderson and Jackson, 1987], followed by hundreds of aftershocks until the beginning of June [De Panfilis and Marcelli, 1968]. In contrast with such high magnitude earthquakes, the Belice Valley does not display any clear morphological evidence of faults, but it is characterized by smooth reliefs expression of large folds. Even after the 1968 earthquake, no surface ruptures or exposed fault scarps along the epicentral zone were observed [Monaco et al., 1996; Barreca et al., 2014; Di Stefano et al., 2015]. Hence, both the identification of seismogenic structures within the Belice area and more in general, the detection of active deformation evidences in southwestern Sicily, are rather challenging.

In this context, the study of the spatial distribution of geochemical anomalies represents a valid additional tool to define and identify active buried structures and areas of active deformation as well. Actually, many studies showed as faults and fractures play a key role in the localization and evolution of geochemical anomalies at the surface [De Gregorio et al., 2002; Finizola et al., 2004; Finizola et al., 2006; Granieri et al., 2006; Werner and Cardellini 2006; Rowland and Simmons, 2012; Brothelande et al., 2014; Cellura et al., 2014; Di Martino et al., 2016; Viveiros et al., 2017]. This is because the migration of fluids through the crust occurs mainly through channels of high permeability generally represented by regional active faults or in sectors under active deformation [Sibson and Rowland, 2003; Fairley and Hinds, 2004; Dogan et al., 2007; Faulkner et al., 2010; Fossen and Rotevatn, 2016]. Thus, the alignment of geochemical anomalies can reveal the presence of preferential ways of rising fluids. In particular soil CO<sub>2</sub> emission has been successfully used to this aim both in volcanic and tectonic settings [De Gregorio et al., 2002; Annunziatellis et al., 2008; Carapezza et al., 2009; Granieri et al., 2010; Granieri et al., 2014; Tarchini et al., 2018; Chiodini et al., 2007; Carapezza et al., 2019]. Generally, the soil CO<sub>2</sub> emission occurs through relatively restricted regions, named diffuse degassing structures (DDS) [Chiodini et al., 2001; Cardellini et al., 2003].

The spatial distribution of DDS in the tectonic context is mainly influenced by the permeability patterns which in turn are guided by tectonic lineament arrangement. Basing on this rationale, we decided to apply the study of the soil CO<sub>2</sub> distributions to detect buried faults and active deformation areas in southwestern Sicily. In particular, we conducted several surveys of the soil CO<sub>2</sub> flux in the surroundings of the area hit by the 1968 seismic sequence, focusing on the sectors with evidence of recent deformations and tectonic structures [Barreca et al., 2014]. Furthermore, the sources of soil CO<sub>2</sub> are investigated through the determination of the isotopic composition of the carbon of soil CO<sub>2</sub>.

## **2. Geological framework**

Western Sicily is a sector of the Sicilian-Maghrebian orogen and is a segment of the Sicilian fold-and-thrust belt (SFTB) (Figure 1). The SFTB is a NE–SW oriented contractional belt including imbrications of Meso-Cenozoic carbonate platform and pelagic successions. The structural architecture of the belt was reconstructed by deep seismic explorations [Catalano et al., 2000 a, b; Finetti et al., 2005]. In southwestern Sicily, the frontal thrust faults show flat-ramp geometries and are still seismically active [Monaco et al., 1996; Morelli and Pondrelli, 1998; DISS Working Group, 2010]. The seismotectonic processes accommodate active compression at the front of the SFTB and particularly along deep-seated thrust planes [Lavecchia et al., 2007; Visini et al., 2010; Sgroi et al., 2012]. On a more detailed scale, the structural setting of the studied area (Figure 1) is characterized by SW-NE and NW-SE trending imbricate thrusts that propagated towards the foreland along Miocene to Quaternary sedimentary horizons (Figure 1). Thrusts propagation was accompanied by the development of large and gentle folds (e.g. Belice Syncline). This shallow thrust and fold system appears trapped between the two structural culminations of Montagna Grande to the north and M. Magaggiaro-Pizzo Telegrafo to the south.

## **3. Soil CO<sub>2</sub> emissions and tectonics**

Natural soil CO<sub>2</sub> emissions represent a substantial part of the carbon emitted in the atmosphere [e.g. Mörner and Etiope, 2002; Burton et al., 2013; Hutchison et al., 2015]. The CO<sub>2</sub> emitted through the soils is generally produced by plants and roots respiration, by the biogenic degradation of organic compounds and the oxidative decay of organic matters [Raich and Potter, 1995; Rastogi et al., 2002; Oertel et al., 2016]. Moreover, in particular areas of the Earth the soil CO<sub>2</sub> emission derive also by the Earth degassing, which consist in the release of CO<sub>2</sub> stored in the crust and in the mantle [Mörner and Etiope, 2002; Fischer, 2008; Dasgupta and Hirschmann, 2010; Burton et al., 2013; Shinohara, 2013; Lee et al., 2016; Zhang et al., 2016].

Earth degassing occurs preferentially in volcanic, geothermal and tectonic areas because several factors promote the deep CO<sub>2</sub> release (e. g. magma ascent, active fault systems, increase of crustal permeability). Among these, the active fault systems play a pivotal role because they represent channels of high permeability allowing the migration of deep-seated fluids through the crust, as observed in a variety of settings [Granieri et al., 2006;



**Figure 1.** Tectonic sketch of the Western Sicily with the location of the investigated areas (A, B, C and D). Tectonic model of the Central Mediterranean (from Barreca et al., [2014]) is shown on the left side.

Aydin, 2000; Savini et al., 2009; Carapezza et al., 2012; Barberi et al., 2013; Foley and Fisher 2017]. Moreover, several papers have demonstrated that the tectonic crustal stress is able to influence fluid circulation [Rowland and Sibson, 2004; Cutillo and Ge, 2006; Wang and Manga, 2010; De Gregorio et al., 2011; Weinlich et al., 2013; Fischer et al., 2014; Padilla et al., 2014; Skelton et al., 2014; Werner et al., 2014; Camarda et al., 2019]

The fault zones are composed of distinct components: (i) a fault core where most of the displacement is accommodated and (ii) an associated damage zone that is mechanically related to the growth of the fault zone [Sibson, 1977; Chester and Logan, 1986; Davison and Wang, 1988; Forster and Evans, 1991; Byerlee, 1993; Scholz and Anders, 1994; Knipe et al. 1998]. The characteristics of fault zones are a function of several factors such as the mechanical properties of the rocks, applied shear strain, fluid-rock interactions, and the state of fracturing. As a result, the permeability of these areas is extremely different and can vary on small spatial scales as a function of burial depth, fault throw, and secondary processes [Fisher and Knipe, 1998; Mailloux et al., 1999; Rawling et al., 2001; Saffer, 2015; Yehya et al., 2018]. Furthermore, the ability to convey fluids is a function of the fault activity. Actually, the fault activation generates fracturing and brecciation of the rock, leading to an increase in permeability. On the contrary, during inactivity period, the fault permeability is reduced by self-sealing phenomena due to the precipitation of hydrothermal fluids [Kennedy et al., 1997; Rowland and Sibson, 2004; Dogan et al., 2007; Burnard et al., 2012; Yehya et al., 2018]. However, faults effectively disrupting the homogeneity of the crust, can act even as barriers to fluid migration [Bense and Person, 2006; Jung et al., 2014].

## 4. Methods

The measurements of soil CO<sub>2</sub> flux were performed using the dynamic concentration method [Gurrieri and Valenza, 1988, Camarda et al., 2006]. This method is based on the measurement of the CO<sub>2</sub> concentration in a

mixture of air and soil gas in a specifically designed probe inserted into the soil to a depth of ~50 cm. The gas mixture inside the probe is obtained by producing a very small negative pressure in the probe using a pump at a constant flux of  $0.8 \text{ L min}^{-1}$ . The mixture is analyzed using an infrared (IR) spectrophotometer connected directly with the probe. After a given time of pump activation [generally less than 1 minute], the value of  $\text{CO}_2$  concentration inside the probe reaches a steady value, this value, named the dynamic concentration  $C_d$ , is proportional to the soil  $\text{CO}_2$  flux [Camarda et al., 2006]. The relationship to convert  $C_d$  values to  $\text{CO}_2$  flux was experimentally deduced by the comparison of  $C_d$  measurements with the values of imposed  $\text{CO}_2$  flux [Camarda et al., 2006]. Several tests were performed using soils with different values of gas permeability and porosity in order to evaluate the influence of soil permeability on the calculated  $\text{CO}_2$  fluxes. These results revealed that the propagated error in the flux calculation is generally less than 5% for soils with gas permeability varying between 0.36 and 123 darcy [Camarda et al., 2006]. The average value of gas permeability for the soils of the Belice Valley is of 3 darcy. This value was calculated on the basis of some gas permeability measurements performed in the investigated area with the *in situ* method described in Camarda et al. [2017].

For isotopic composition analyses, the soil gases were sampled at a depth of 50 cm through a 5 mm diameter Teflon tube connected to a syringe and then stored in glass flasks equipped with vacuum stopcocks. The isotopic composition of  $\text{CO}_2$  carbon was measured using a Finnigan Mat Delta Plus Mass Spectrometer. The isotopic values are expressed as  $\delta^{13}\text{C}$  in per mill (‰) versus the Vienna Pee Dee Belemnite (V-PDB) standard, the uncertainty is  $\pm 0.2\text{‰}$ .

## 5. Results and discussion

Depending on the structural context, we adopted two different investigation strategies. In detail, for the areas where evidences of active deformation and tectonic structures are available, we performed the measurements along some profiles crossing their traces (area A, B, and C in Figure 1). Where no superficial evidence of faults are known, such as in the area of Belice Valley (area D in Figure 1) hit by 1968 seismic sequences, we made a larger survey carrying out measurements on a mesh of homogeneously distributed points. To investigate the origin of soil  $\text{CO}_2$ , in several selected sites we sampled soil gas to analyze the carbon isotopic composition of  $\text{CO}_2$ .

### 5.1 Artificial basin of the Garcia dam

The first investigated area is placed close to the artificial basin of the Garcia dam, 5 km NE of Belice main shock epicentral area (area A in Figure 1), where Barreca et al. [2014] reported evidence of active deformation.

In particular, they found along the road skirting the artificial basin, a concrete side-wall displaced by a W-E trending reverse fault. Basing on the geomorphological survey, these authors infer that observed ground deformation is the result of tectonic creep, excluding the origin from surface gravitational processes. In this site, we performed 10 measurements perpendicular to ground deformation trace, distributed over a length of about 1 km (Figure 2). The measurements were performed on September 4, 2014, one day after the occurrence of a seismic event with  $M 2.9$  about 3 km NE of the investigated area (Figure 2). This concurrence put us in the most favorable conditions to study the relationship between tectonic and soil  $\text{CO}_2$  flux. Actually, it was observed that release of soil  $\text{CO}_2$  can increase in response to tectonic stress related to the seismic activity [Padilla et al., 2014; Werner et al., 2014; Camarda et al., 2016; Hernández et al., 2017; Camarda et al. 2019]. Due to the limited length of the profile, we have been able to carry out the measurements in the same type of soils with homogeneous vegetation. The measured soil  $\text{CO}_2$  flux values ranged from 4 to  $23 \text{ g m}^{-2} \text{ d}^{-1}$  (Table 1).

These values fall within the range ( $0.2 \div 21 \text{ g m}^{-2} \text{ d}^{-1}$ ) of typical soil  $\text{CO}_2$  emissions measured in a variety of ecosystems [Raich and Schlesinger; 1992; Raich and Tufekcioglu, 2000]. This feature seems to suggest the absence of any supply of deep  $\text{CO}_2$  related to the deformation zone. Nevertheless, considering the homogeneity of the vegetation, the range of measured values is quite wide with a coefficient of variation of 0.46 (Table 1). Furthermore, it is worth noting that the arrangement of values along the profile was not random, but rather showed a decreasing trend progressively moving away from the active deformation area (Figure 2). These last two elements suggest that a preferential release of  $\text{CO}_2$  occurred near the ground deformation area.

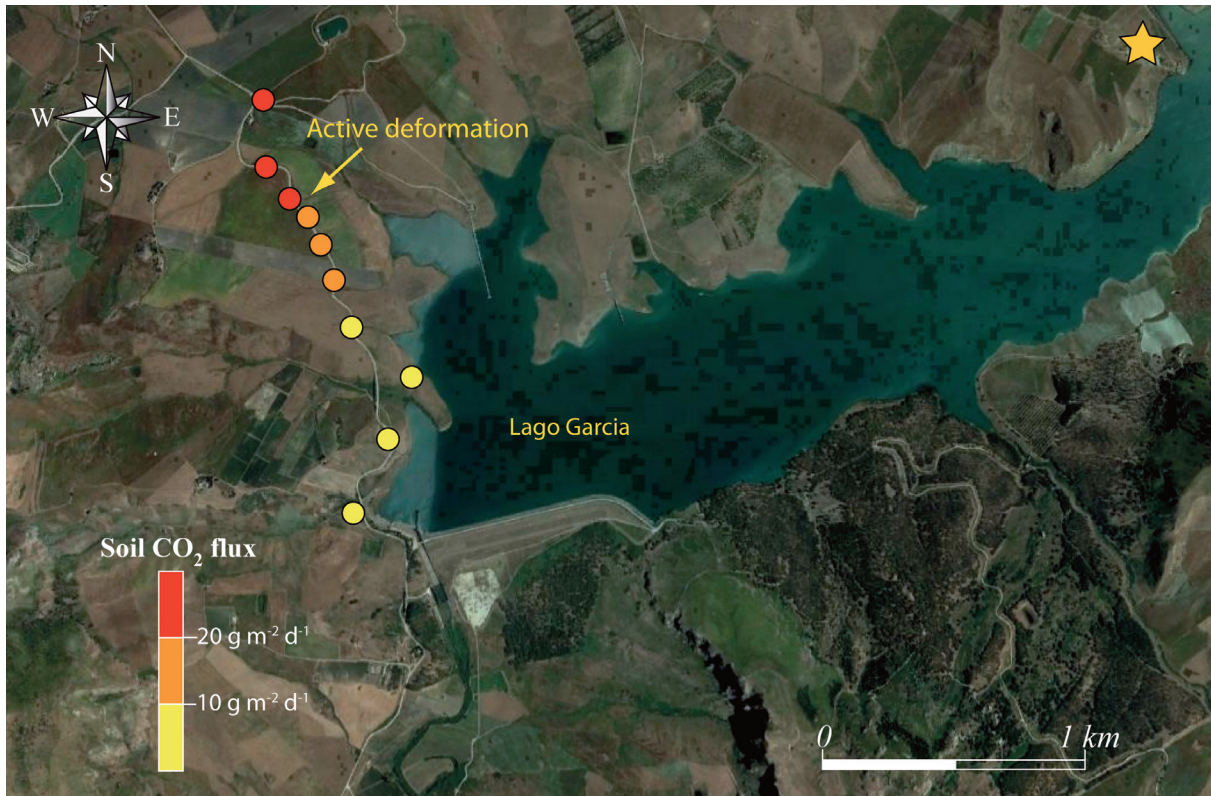


**Figure 2.** Spatial pattern of the soil CO<sub>2</sub> flux along a profile close to the Garcia dam, where an active deformation area was recognized by Barreca et al. [2014]. The yellow star shows the location of seismic event with  $M 2.9$  occurred one day before flux survey.

Area	Min (g m <sup>-2</sup> d <sup>-1</sup> )	Max (g m <sup>-2</sup> d <sup>-1</sup> )	Mean flux (g m <sup>-2</sup> d <sup>-1</sup> )	CV
Garcia dam	4	23	13	0.46
Santa Ninfa	4	162	61	0.87
Castelvetrano	6	50	21	0.45
Belice Valley	1	430	47	1.53

**Table 1.** Summary statistics for CO<sub>2</sub> flux data

## 5.2 Santa Ninfa karst system

Santa Ninfa karst system is placed on a wide plateau characterized by the presence of gypsum rocks. It develops along the main fault system of the area (area B in Figure 1). The hypogean system consists of pseudo-orthogonal grids of cavities whose orientations follow the trends of the main tectonic structures. In this area, we performed 12 measurements along a profile about 2 km long. The profile follows the main road passing over the Santa Ninfa karst system (Figure 3). The mean value of soil CO<sub>2</sub> flux is the highest measured among the studied areas (61 g m<sup>-2</sup> d<sup>-1</sup>, Table 1). The lowest values of soil CO<sub>2</sub> flux were recorded in the three points placed just above the karst system, whereas the measured soil CO<sub>2</sub> flux was above the threshold value due to organic production (21 g m<sup>-2</sup> d<sup>-1</sup>) in the residual part of the profile.

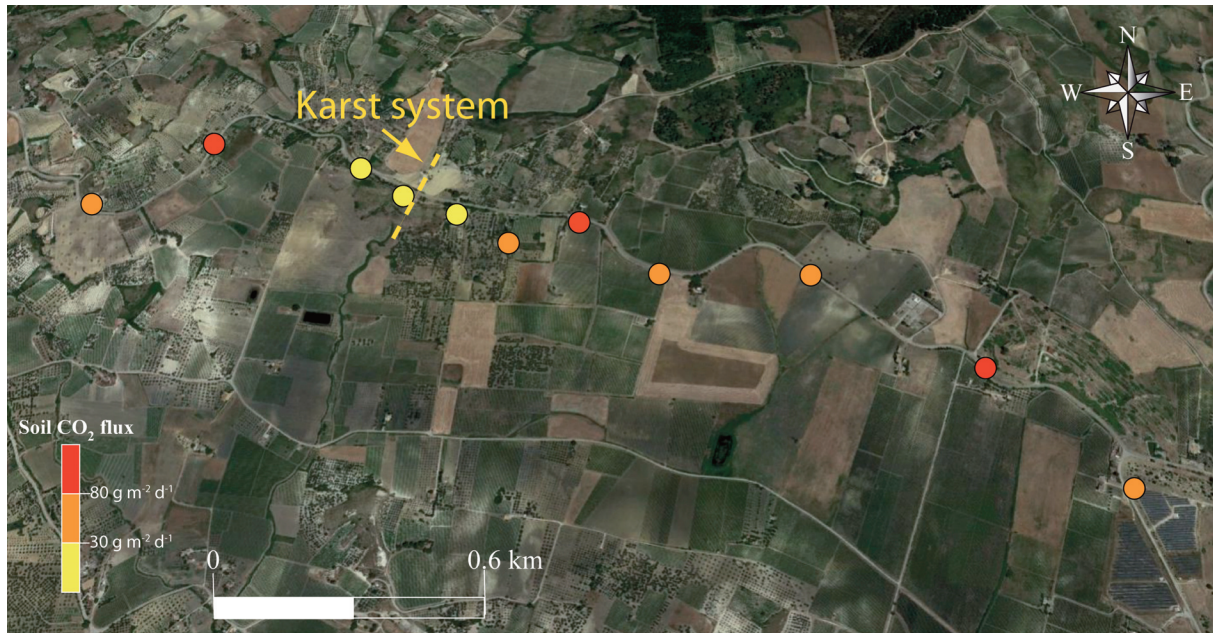


**Figure 3.** Spatial pattern of the soil CO<sub>2</sub> flux along a profile crossing the Santa Ninfa karst system (indicated by the dashed yellow line).

The high values of the soil CO<sub>2</sub> flux found in this area reveal the occurrence of a preferential discharge of deep-seated fluids. At the same time, the lowest values recorded just above the S. Ninfa karst system, show how the superficial structure acts as a sink for the CO<sub>2</sub>, decreasing the soil CO<sub>2</sub> flux at the surface.

### 5.3 Castelvetroano ancient settlements

The third investigated area is placed south of Castelvetroano town (area C in Figure 1), in an area of intense active deformation developing along the Campobello di Mazara–Castelvetroano alignment. Interferometric SAR data reveal up to 2 mm/yr differential ground motion [Barreca et al., 2014] along this alignment. We performed soil CO<sub>2</sub> flux measurements near the surface evidence of a reverse SSW–NNE trending fault which cuts an ancient settlement [Barreca et al., 2014]. We made 22 soil CO<sub>2</sub> flux measurements along several transects crossing the ancient settlement (Figure 4)

The CO<sub>2</sub> flux values ranged from 6 to 50 g m<sup>-2</sup> d<sup>-1</sup>. In four points, the soil CO<sub>2</sub> values were above the typical soil CO<sub>2</sub> values due to exclusively organic production (21 g m<sup>-2</sup> d<sup>-1</sup>) pointing out the presence of an additional source of CO<sub>2</sub> with respect to the solely biogenic one. Interestingly, the spatial distribution of soil CO<sub>2</sub> flux values (Figure 4) reveals how the highest values were found along the trace of the most evident surface deformation (Figure 4).

### 5.4 Belice valley

In the Belice Valley area, we performed 100 measurements following a grid of points evenly distributed, covering a surface of about 20 km<sup>2</sup>. In particular, we focused on an area placed 10 km southeast from the mainshock epicentral area, including the NE portion of Belice Valley (area D in Figure 1). The range of the measured soil CO<sub>2</sub> flux is very wide, ranging from 1 to 430 g m<sup>-2</sup> d<sup>-1</sup> with a coefficient of variation of 1.53 (Table 1).

Many measurement sites were characterized by soil CO<sub>2</sub> flux values well above the threshold value for a CO<sub>2</sub> produced by the organic processes. The large variability of soil CO<sub>2</sub> flux and the elevated measured values indicate

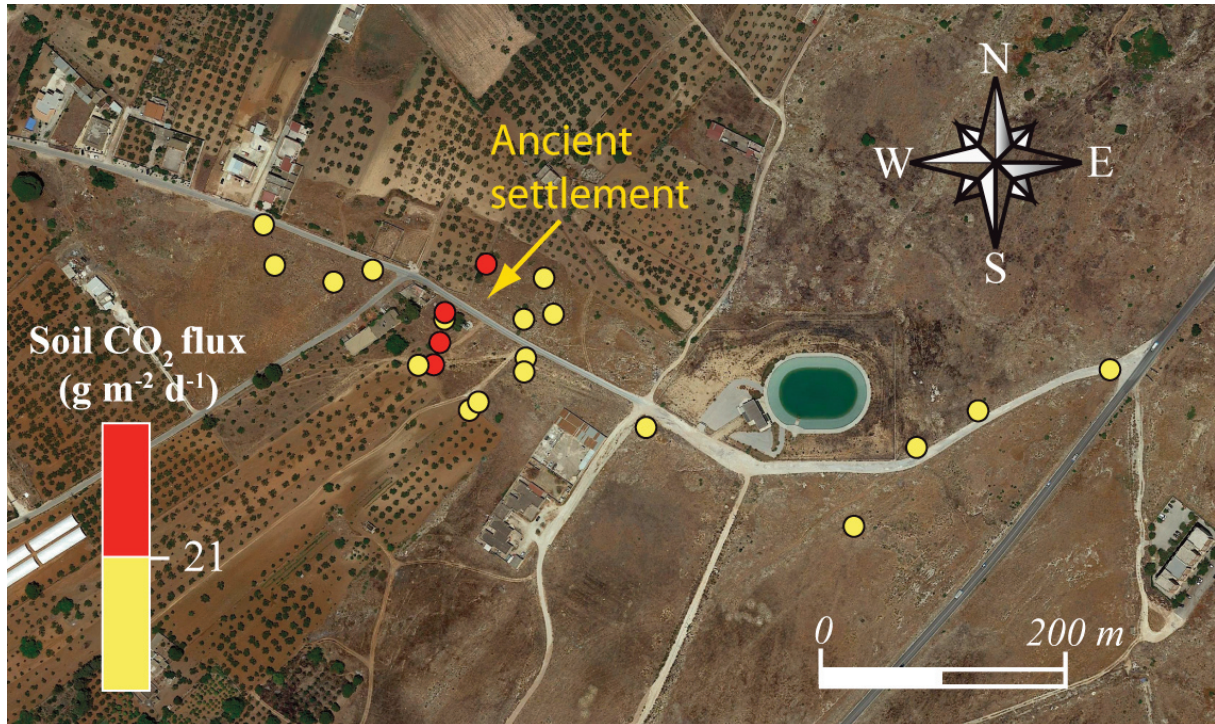


Figure 4. Spatial pattern of the soil CO<sub>2</sub> flux in some profiles close the Castelvetrano ancient settlements.

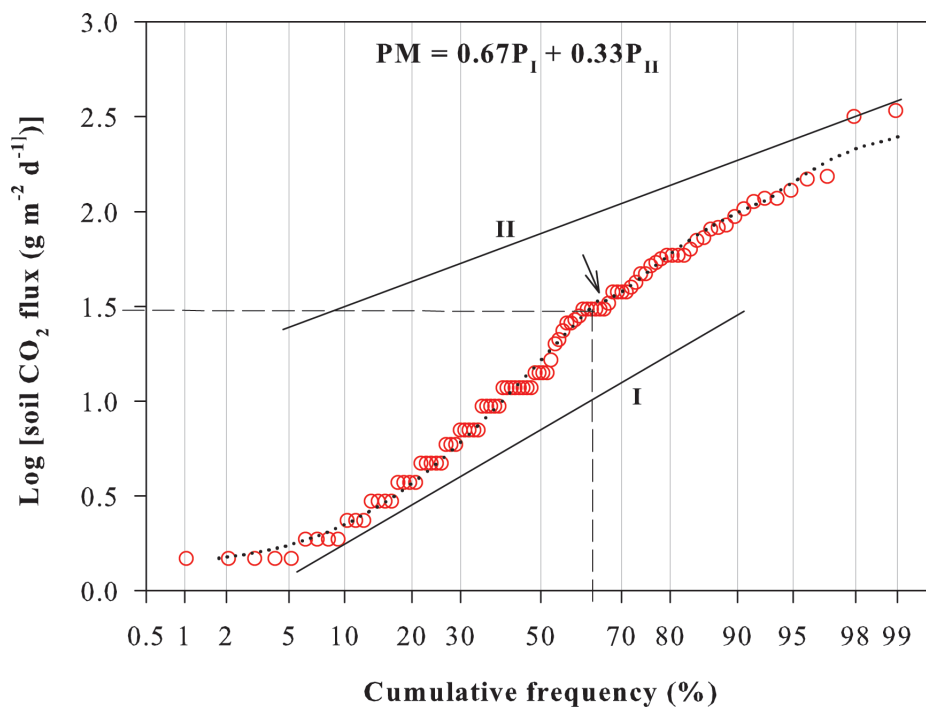


Figure 5. Probability plot of soil CO<sub>2</sub> fluxes measured on the Belice Valley area. Dotted line shows the theoretical distribution produced by combining the populations in the proportions indicated by the threshold values (black arrows) according to the equation reported at the top of each graph. Solid lines indicate the populations reconstructed according to the procedure illustrated by Sinclair [1974].

the presence of several sources of CO<sub>2</sub>. Hence, the Normal Probability Plot (NPP) [Sinclair, 1974; Chiodini et al., 2008] has been used to identify the populations of data ascribable to different origins.

This plot shows the probabilities of cumulative frequencies of the measured soil CO<sub>2</sub> fluxes. In this type of plot, the inflection points indicate the different normally distributed populations composing the dataset (+1 overlapping populations would result in a curve characterized by n inflection points). The NPP in Figure 5, shows one inflection point and hence indicates the presence of two different populations. The inflection point represents the threshold value separating the populations.

The estimated threshold for this survey corresponds to a soil CO<sub>2</sub> flux value of 30 g m<sup>-2</sup> d<sup>-1</sup>. To check the validity of the two-population model, we compared the theoretical distribution resulting from the combination of the portioned populations (dotted line in Figure 5) with the actual data distribution (open red circles in Figure 5). The actual and theoretical distributions are in agreement thus proving the validity of the proposed two-population model. Being the threshold value of 30 g m<sup>-2</sup> d<sup>-1</sup> close to the highest value reported for a CO<sub>2</sub> of organic origin (21 g m<sup>-2</sup> d<sup>-1</sup>), it can be inferred that the population I, with a mean value of 7 g m<sup>-2</sup> d<sup>-1</sup>, is representative of an organic CO<sub>2</sub> source, deriving from the microbial decomposition of organic soil matter and root respiration. The population II displayed values above 30 g m<sup>-2</sup> d<sup>-1</sup> up to a maximum value of 430 g m<sup>-2</sup> d<sup>-1</sup> and with a mean value of 75 g m<sup>-2</sup> d<sup>-1</sup>. This last population represents 33% of all the measurements and it can be considered representative of a deep CO<sub>2</sub> source. To investigate the spatial distribution of soil CO<sub>2</sub>, we processed the data using two different geostatistical methods. Firstly, we applied Kriging interpolation [Swan & Sandilands, 1995] to obtain a soil CO<sub>2</sub> flux map showing the spatial distribution and the extent of the areas with anomalous soil CO<sub>2</sub> flux (i.e. flux above the previously identified threshold value of 30 g m<sup>-2</sup> d<sup>-1</sup>). The map in Figure 6A, shows as at least one-third of the area displayed values above 30 g m<sup>-2</sup> d<sup>-1</sup>, and further evidence as the anomalous areas are mainly aligned along with two main perpendicular directions SW-NE and NW-SE. Furthermore, the anomaly placed in the central part of the investigated area extends along an E-W direction.

Once ascertained the existence of consistent anomalous degassing areas, we applied the sequential Gaussians simulation (sGs) method to rigorously define the existence of diffusive degassing structures (DDS) and preferential alignments linked to anomalous soil CO<sub>2</sub> emissions. This method is widely used to study soil diffuse degassing processes in volcanic-hydrothermal environments [e.g. Lewicki et al., 2003; Chiodini et al., 2004; Frondini et al., 2004; Caliro et al., 2005; Fridrikson et al., 2006; Granieri et al., 2006; Werner and Cardellini, 2006; Chiodini et al., 2007; Padròn et al., 2008; Werner et al., 2008; Viveros et al., 2017]. The main advantage of this method is that it does not attenuate the extreme values and allows the estimation of the uncertainty [Cardellini et al., 2003]. The sGs method consists in producing numerous simulations of the spatial distribution of the attribute (CO<sub>2</sub> flux, in our case) and is carried out using the algorithm described by Deutsch and Journel [1998]. We performed the sGs by means of the Stanford Geostatistical Modeling Software (SGeMS), an open-source package developed for solving problems involving spatially related variables. To perform sGs following the methods of Cardellini et al. [2003], we normalized CO<sub>2</sub> flux data and subsequently we examined the spatial variability of the measured soil CO<sub>2</sub> fluxes using the semivariogram of normalized data. For the visualization of the result of the simulations, we elaborate a probability map, in which is displayed the probability that each grid of the sGs exceeds a threshold value of soil CO<sub>2</sub> flux. According to Cardellini et al., [2003] to define the extent of the active DDS we used as threshold, the value splitting the two soil CO<sub>2</sub> population in the NPP [i.e. 30 g m<sup>-2</sup> d<sup>-1</sup>]. The probability maps are very similar to that one obtained by Kriging interpolation but better define the presence of some DDS (red areas in Figure 6B). The DDSs are preferentially elongated along with two perpendicular directions SW-NE and NW-SE respectively. These directions are in agreement with the orientation of the main tectonic structures (white dotted lines) recognized in the area [Barreca et al., 2014; Di Stefano et al., 2015].

## **5.5 Origin of CO<sub>2</sub>**

The results of soil CO<sub>2</sub> investigation, in particular the NPP results, point out the presence of at least two different CO<sub>2</sub> sources. To investigate the different CO<sub>2</sub> sources, we sampled the soil gas to determine the carbon isotopic composition of CO<sub>2</sub> in the sites with the highest values of soil CO<sub>2</sub> flux. In particular, three samples were collected in Castelevetrano ancient settlement area, two samples in the S. Ninfa karst system, and 9 samples

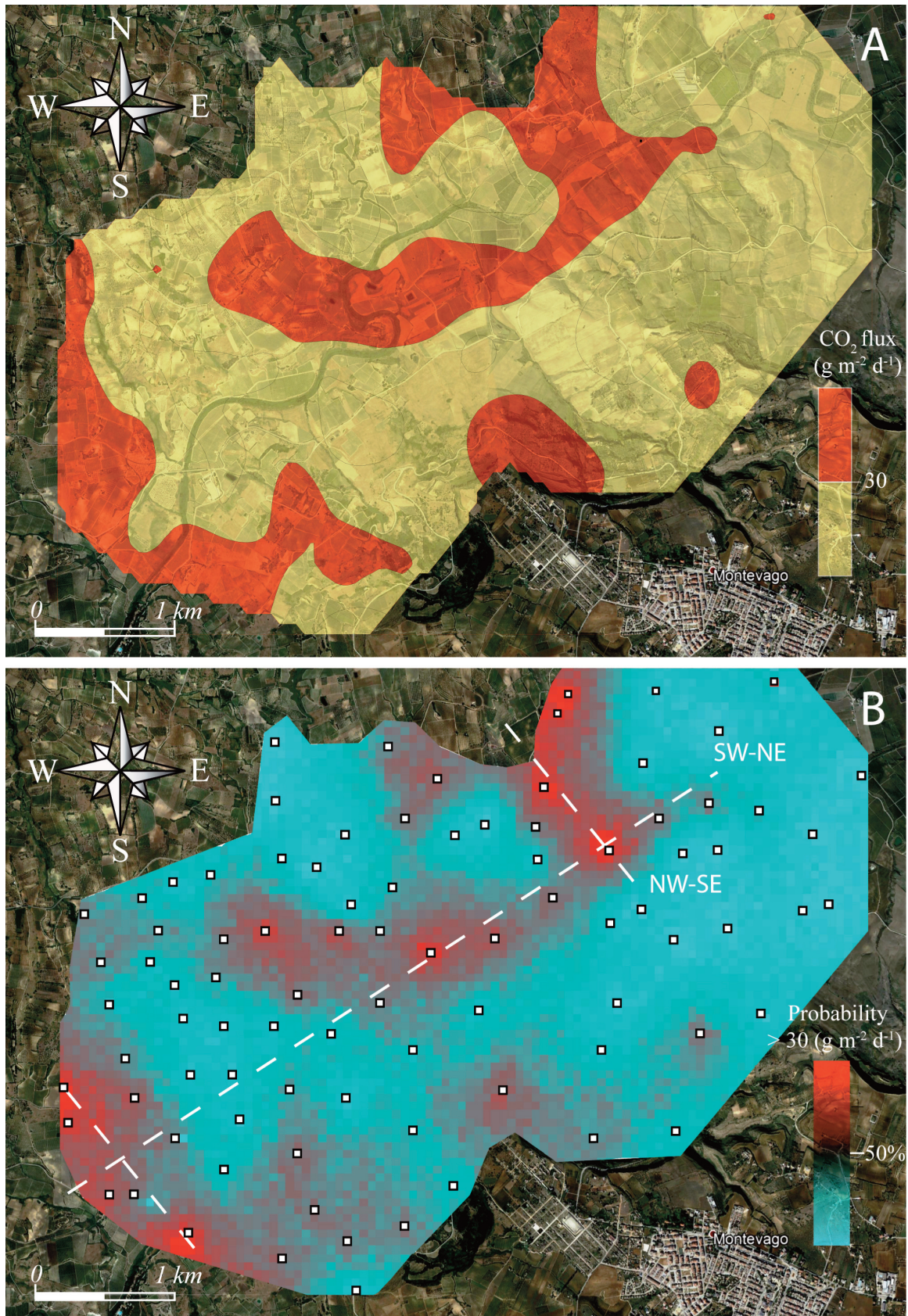


**Figure 6.** A: map of the spatial distribution of the soil CO<sub>2</sub> flux at the Belice Valley area; B: probability maps of soil CO<sub>2</sub> flux at the Belice Valley area; colour scale on map B shows the probability of soil CO<sub>2</sub> flux exceeding 30 g m<sup>-2</sup> d<sup>-1</sup>; dotted white lines on map B show the main directions of elongation of the flux anomalies (DDS); with squares show the measurement points.

in the Belice Valley area. The values of  $\delta^{13}\text{C}(\text{CO}_2)$  ranged between  $-15\text{‰}$  and  $-25\text{‰}$ . To evidence the occurrence of mixing processes between  $\text{CO}_2$  of different origins we used the  $\delta^{13}\text{C}$  values vs the  $\text{CO}_2$  concentration and the  $\delta^{13}\text{C}$  values vs the soil  $\text{CO}_2$  flux plots (Figures 7A and 7B).

In Figure 7A we drove: (i) theoretical curves of mixing between air  $\text{CO}_2$  and organic production  $\text{CO}_2$  and (ii) theoretical curves for mixing between organic production  $\text{CO}_2$  and deep origin  $\text{CO}_2$ . For the air end-member, we used a  $\delta^{13}\text{C} = -8\text{‰}$  and  $\text{CO}_2$  concentration of 440 ppm. For organic end-members, we used two  $\delta^{13}\text{C}$  values of  $-22\text{‰}$  and  $-26\text{‰}$ . The isotopic value of the upper limit for organic endmembers ( $-22\text{‰}$ ) corresponds to the highest value of the typical range for bulk organic carbon of  $\text{C}_3$  plants [O’Leary, 1988]. We excluded the more positive values due to  $\text{CO}_2$  derived from  $\text{C}_4$  plants because all measurements were performed in sites without this type of vegetation (e.g. maize, sorghum, sugarcane). For deep origin  $\text{CO}_2$  we used: [i] the two extreme values for mantellic origin reported in the literature,  $-5\text{‰}$  and  $-8\text{‰}$  respectively [Taylor, 1986] and the value of  $0\text{‰}$  for  $\text{CO}_2$  produced by decarbonation process. It is important to point out that despite being in a non-volcanic context we have used however typical mantellic end members because, for the area, Caracausi et al. [2005] detected high mantle-helium fluxes. The majority of points lie along the last part of mixing lines between air  $\text{CO}_2$  and organic origin ones. In particular, the values fall very close to the organic end-member values revealing a very low contribution of air  $\text{CO}_2$  in the soil gas. The three samples collected in the Castelvetrano area fall outside this general trend. They, more likely, lie along the mixing lines between mantellic-organic sources.

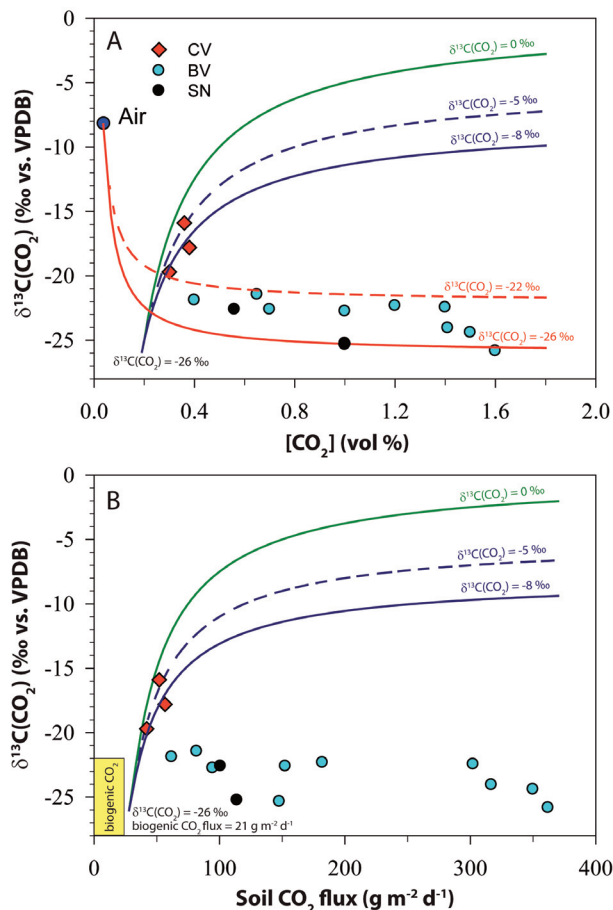


**Figure 7.** Plot of  $\delta^{13}\text{C}(\text{CO}_2)$  versus soil  $\text{CO}_2$  concentration (plot A) and soil  $\text{CO}_2$  flux (plot B) relative to some gas samples collected at Castelvetrano (CV), Santa Ninfa (SN) and Belice Valley (BV); green curve: mixing between a biogenic and a deep  $\text{CO}_2$  with  $\delta^{13}\text{C}(\text{CO}_2) = 0\text{‰}$ ; dashed blue curve: mixing between a biogenic and a deep  $\text{CO}_2$  with  $\delta^{13}\text{C}(\text{CO}_2) = -5\text{‰}$ ; blue curve: mixing between a biogenic and a deep  $\text{CO}_2$  with  $\delta^{13}\text{C}(\text{CO}_2) = -8\text{‰}$ ; dashed red curve: mixing between air and a biogenic  $\text{CO}_2$  with  $\delta^{13}\text{C}(\text{CO}_2) = -22\text{‰}$ ; red curve: mixing between air and a biogenic  $\text{CO}_2$  with  $\delta^{13}\text{C}(\text{CO}_2) = -26\text{‰}$ . The yellow box in plot B indicates the range of flux and  $\delta^{13}\text{C}(\text{CO}_2)$  values typical of the shallow biogenic  $\text{CO}_2$ .

In Figure 7B we plotted the mixing curves between deep CO<sub>2</sub> and organic production CO<sub>2</sub> with a flux value of 21 g m<sup>-2</sup> d<sup>-1</sup>. We reported the soil CO<sub>2</sub> flux field due to organic production. The points of Castelvetro area are again well aligned along the curves of mixing between mantle and organic CO<sub>2</sub> end-member, confirming a deep CO<sub>2</sub> supply for this area. The remaining points, though with an isotopic marker typical of organic CO<sub>2</sub> production, fall well outside the field of typical soil CO<sub>2</sub> flux of organic shallow production. It is reasonable to suppose for these sites a deep supply of crustal origin because large volumes of carbon dioxide (up to 90%) have been encountered in sedimentary basins from various geological settings [Wycherley et al., 1999]. Indeed, the CO<sub>2</sub> from the crustal origin, besides an origin due to the above mentioned decarbonation reactions, can derive also from: thermogenic breakdown of organic matter in buried sediments, thermal maturation of kerogen, biogenic breakdown of oil and gas [Ni et al., 2014; Dai et al., 2012]. The isotopic composition of these last types of crustal CO<sub>2</sub> is rather wide: +10‰ ÷ -30‰ [e.g. Whiticar, 1994; Ni et al., 2014]. The values due to organic production CO<sub>2</sub> in soil layers fall in this wide range. Hence, the isotopic composition of this crustal CO<sub>2</sub> is compatible with the measured values, supporting the hypothesis of a crustal origin for the gases of the Belice Valley area.

## 6. Conclusions

The soil CO<sub>2</sub> flux values measured in a large number of points of the studied area were above the typical range of values due to a simple organic CO<sub>2</sub> production, revealing a deep supply of CO<sub>2</sub> in the Belice Valley area. The isotopic composition data of carbon of the soil CO<sub>2</sub> are in agreement with this evidence. However, our data do not univocally distinguish between the mantle or crustal origin of the supply. Nevertheless, the spatial pattern of soil CO<sub>2</sub> emission resulted strongly influenced by the presence of tectonic structures and active crustal deformations in the area. In detail, in the Belice Valley area, the spatial distribution of the soil CO<sub>2</sub> flux was not random but it revealed the presence of DDSs elongated in the SW-NE and NW-SE directions, in agreement with the main tectonic feature of the area, pointing out the presence of active buried structure beneath Belice Valley.

The measurements performed in the areas with evidence of active deformations shown as the CO<sub>2</sub> is preferentially released in correspondence of the morphological evidence of the traces of active deformations.

**Acknowledgements.** We wish to thank two anonymous reviewers whose comments greatly improved the manuscript.

## References

- Anderson, H. and J. Jackson (1987). Active tectonics in the Adriatic region, *Geophys. J. R. Astron. Soc.*, 91, 937-983.
- Annunziatellis, A., S.E. Beaubien, S. Bigi, G. Ciotoli, M. Coltella and S. Lombardi (2008). Gas migration along fault systems and through the vadose zone in the Latera caldera (central Italy): implications for CO<sub>2</sub> geological storage, *Int. J. of Greenhouse Gas Control*, 2, 353-372.
- Aydin, A. (2000). Fractures, faults, and hydrocarbon entrapment, migration and flow, *Mar. Petrol. Geol.*, 17, 797-814, [https://doi.org/10.1016/S0264-8172\(00\)00020-9](https://doi.org/10.1016/S0264-8172(00)00020-9).
- Barberi, F., M. L. Carapezza, R. Cioni, M. Lelli, M. Menichini, M. Ranaldi, T. Ricci, L. Tarchini, (2013). New geochemical investigations in Platanares and Azacualpa geothermal sites (Honduras), *J. Volcanol. Geotherm. Res.*, 257, 113-134.
- Barreca, G., V. Bruno, C. Cocorullo, F. Cultrera, L. Ferranti, F. Guglielmino, L. Guzzetta, M. Mattia, C. Monaco and F. Pepe (2014). Geodetic and geological evidence of active tectonics in south-western Sicily (Italy), *J. Geodyn.*, 82, 138-149.
- Bense, V.F. and M.A. Person (2006). Faults as conduit-barrier systems to fluid flow in siliciclastic sedimentary aquifers, *Water Resour. Res.*, 42, W05421. <https://doi.org/10.1029/2005WR004480>.
- Brothelande, E., A. Finizola, A. Peltier, E. Delcher, J.C. Komorowski, F. Di Gangi, G. Borgogno, M. Passarella, C. Trovato and Y. Legendre (2014). Fluid circulation pattern inside La Soufrière volcano (Guadeloupe) inferred from combined electrical resistivity tomography, self-potential, soil temperature and diffuse degassing

- measurements, *J. Volcanol. Geotherm. Res.*, 288, 105-122.
- Burnard, P., S. Bourlange, P. Henry, L. Geli, M.D. Tryon, B. Natal'in, A.M.C. Sengör, M.S. Özeren and M.N. Çagatay (2012). Constraints on fluid origins and migration velocities along the Marmara Main Fault (Sea of Marmara, Turkey) using helium isotopes, *Earth Planet. Sci. Lett.*, 341, 68-78, <https://doi.org/10.1016/j.epsl.2012.05.042>.
- Burton, M.R., G.M. Sawyer and D. Granieri (2013). Deep Carbon Emissions from Volcanoes, *Rev. Mineral. Geochem.*, 75, 323-354.
- Byerlee, W.F. (1993). Model for Episodic Flow of High-pressure Water in Fault Zones before Earthquakes, *Geology*, 21, 303-306.
- Caliro, S., G. Chiodini, R. Avino, C. Cardellini and F. Frondini (2005). Volcanic degassing at Somma-Vesuvio (Italy) inferred by chemical and isotopic signatures of ground water, *Appl. Geochem.*, 20, (6), 1060-1076.
- Camarda, M., S. De Gregorio, G. Capasso, R.M.R. Di Martino, S. Gurrieri and V. Prano (2019). The monitoring of natural soil CO<sub>2</sub> emissions: Issues and perspectives. *Earth-Science Reviews* 198, 2019, 102928.
- Camarda, M., V. Prano, S. Cappuzzo, S. Gurrieri and M. Valenza (2017). Temporal variations in air permeability and soil CO<sub>2</sub> flux in volcanic ash soils (island of Vulcano, Italy). *Geochem. Geophys. Geosyst.* 18, 3241-3253.
- Camarda, M., S. De Gregorio, R.M.R. Di Martino and R. Favara (2016). Temporal and spatial correlations between soil CO<sub>2</sub> flux and crustal stress, *J. Geophys. Res. Solid Earth*, 121, 7071-7085, doi:10.1002/2016JB013297.
- Camarda, M., S. Gurrieri and M. Valenza (2006). CO<sub>2</sub> flux measurements in volcanic areas using the dynamic concentration method: Influence of soil permeability, *J. Geophys. Res.*, 111, B05202. <https://doi.org/10.1029/2005JB003898>.
- Caracausi, A., R. Favara, F. Italiano, P.M. Nuccio, A. Paonita and A. Rizzo (2005). Active geodynamics of the central Mediterranean Sea: Tensional tectonic evidences in western Sicily from mantle-derived helium, *Geophys. Res. Lett.*, 32, L04312, <https://doi.org/10.1029/2004GL021608>.
- Carapezza, M.L., F. Barberi, M. Ranaldi, L. Tarchini and N.M. Pagliuca (2019). Faulting and Gas Discharge in the Rome Area (Central Italy) and Associated Hazards, *Tecnica*, 38, 941-959, <https://doi.org/10.1029/2018TC005247>.
- Carapezza, M.L., F. Barberi, M. Ranaldi, T. Ricci, L. Tarchini, J. Barrancos, C. Fischer, D. Granieri, C. Lucchetti, G. Melian, N. Pérez, P. Tuccimei, A. Vogel and K. Weber (2012). Hazardous gas emissions from the flanks of the quiescent Colli Albani volcano (Rome, Italy), *Appl. Geochem.*, 27, (9), 1767-1782, <https://doi.org/10.1016/j.apgeochem.2012.02.012>.
- Carapezza, M.L., T. Ricci, M. Ranaldi and L. Tarchini (2009). Active degassing structures of Stromboli and variation of the diffuse CO<sub>2</sub> output related to the volcanic activity, *J. Volcanol. Geotherm. Res.*, 182, 231-245.
- Cardellini, C., G. Chiodini and F. Frondini (2003). Application of stochastic simulation to CO<sub>2</sub> flux from soil: mapping and quantification of gas release. *J. Geophys. Res.*, 108, 2425, <https://doi.org/10.1029/2002JB002165>.
- Catalano, R., A. Franchino, S. Merlini and A. Sulli (2000a). Central western Sicily structural setting interpreted from seismic reflection profiles, *Mem. Soc. Geol. Ital.*, 55, 5-16.
- Catalano, R., A. Franchino, S. Merlini, and A. Sulli (2000b). A crustal section from the Eastern Algerian basin to the Ionian ocean (Central Mediterranean), *Mem. Soc. Geol. Ital.*, 55, 71-85.
- Cellura, D., V. Stagno, M. Camarda and M. Valenza (2014). Diffuse soil CO<sub>2</sub> degassing from Linosa island, *Ann. Geophys.*, 57, 3, S0329.
- Chester, F.M. and J.M. Logan (1986). Implications for mechanical properties of brittle faults from observations of the Punchbowl fault zone, California, *Pure App. Geophys.*, 124, 77-106.
- Chiodini, G., S. Caliro, C. Cardellini, R. Avino, D. Granieri and A. Schmidt (2008). Carbon isotopic composition of soil CO<sub>2</sub> efflux, a powerful method to discriminate different sources feeding soil CO<sub>2</sub> degassing in volcanic-hydrothermal areas, *Earth Planet. Sci. Lett.*, 274, (3-4), 372-379, <https://doi.org/10.1016/j.epsl.2008.07.051>.
- Chiodini, G., A. Baldini, F. Barbieri, M.L. Carapezza, C. Cardellini, F. Frondini, D. Granieri and M. Ranaldi (2007). Carbon dioxide degassing at Latera caldera (Italy): evidence of geothermal reservoir and evaluation of its potential energy, *J. Geophys. Res.*, 112, B12204.
- Chiodini, G., R. Avino, T. Brombach, S. Caliro, C. Cardellini, S. De Vita, F. Frondini, E. Marotta and G. Ventura (2004). Fumarolic degassing west of Mount Epomeo, Ischia (Italy), *J. Volcanol. Geotherm. Res.*, 133, 291-309.
- Chiodini, G., F. Frondini, C. Cardellini, D. Granieri, L. Marini and G. Ventura (2001). CO<sub>2</sub> degassing and energy release at Solfatara volcano, Campi Flegrei, Italy, *J. Geophys. Res.*, 106, 16213-16221.
- Cuttillo, P.A. and S. Ge (2006). Analysis of strain-induced ground-water fluctuations at Devils Hole, Nevada, *Geofluids*,

- 6, 319–33.
- Dai, J., Y. Ni and C. Zou C. (2012). Stable carbon and hydrogen isotopes of natural gases sourced from the Xujiahe Formation in the Sichuan Basin, China, *Org. Geochem.*, 43, 103–111.
- Dasgupta, R. and M. Hirschmann (2010). The deep carbon cycle and melting in Earth's interior, *Earth Planet. Sci. Lett.*, 298, 1–13.
- Davison, C. C. and C. Y. Wang, (1988). Hydrogeologic characteristics of major fracture zones in a large granite batholith of the Canadian shield, in *Proceedings, 4th Canadian-American Conference on Hydrogeology*, Banff, Canada, June 1988.
- De Gregorio, S., C. Federico, S. Cappuzzo, R. Favara, G. Giudice, S. Gurrieri and E. Boschi (2011). Stress-induced temperature variations in groundwater of the Monferrato area (north-western Italy), *Geofluids*, 12, 142–149. <https://doi.org/10.1111/j.1468-8123.2011.00348.x>.
- De Gregorio, S., I.S. Diliberto, S. Giammanco, S. Gurrieri and M. Valenza (2002). Tectonic control over large-scale diffuse degassing in eastern Sicily (Italy), *Geofluids*, 2, 273–284.
- De Panfilis, M. and L. Marcelli (1968). Il periodo sismico della Sicilia orientale iniziato il 14/1/1968, *Ann. Geofis.*, 21, 343–422.
- Di Martino, R.M.R., G. Capasso, M. Camarda (2016). Spatial domain analysis of carbon dioxide from soils on Vulcano Island: Implications for CO<sub>2</sub> output evaluation, *Chem. Geol.*, 444, 59–70.
- Di Stefano, P., R. Favara, D. Luzio, P. Renda, M.S. Cacciatore, M. Calò, G. Napoli, L. Parisi, S. Todaro, and G. Zarcone (2015). A regional-scale discontinuity in western Sicily revealed by a multidisciplinary approach: A new piece for understanding the geodynamic puzzle of the southern Mediterranean, *Tectonics*, 34, 2067–2085.
- DISS Working Group, Data Base of Individual Seismogenic Sources: A compilation of potential sources for earthquakes larger than M 5.5 in Italy and surrounding areas, (2010). <http://diss.rm.ingv.it/diss/>, © INGV 2010.
- Deutsch, C. V. and A. G. Journel (1998), *GSLIB: Geostatistical Software Library and Users Guide*, 369 pp., Oxford Univ. Press, New York.
- Dogan, T., T. Mori, F. Tsunomori and K. Notsu (2007). Soil H<sub>2</sub> and CO<sub>2</sub> surveys at several active faults in Japan, *Pure Appl. Geophys.*, 164, 2449–2463.
- Fairley, J.P. and J.J. Hinds (2004). Rapid transport pathways for geothermal fluids in an active Great Basin fault zone, *Geology*, 32, 9, 825–828.
- Faulkner, D.R., C.A. L. Jackson, R.J. Lunn, R.W. Schlische, Z.K. Shipton, C.A.J. Wibberley and M.O. Withjack, (2010). A review of recent developments concerning the structure, mechanics and fluid flow properties of fault zones, *J. Struct. Geol.*, 32, 1557–1575.
- Finetti, I.R., F. Lentini, S. Carbone, A. Del Ben, A. Di Stefano, E. Forlin, P. Guarnieri, M. Pipan and A. Prizzon (2005). Geological outline of Sicily and Lithospheric Tectonodynamics of its Tyrrhenian Margin from new CROP seismic data. In: Finetti, I.R. (Ed.), *CROP PROJECT: Deep Seismic Exploration of the Central Mediterranean and Italy*. Elsevier.
- Finizola, A., A. Revil, E. Rizzo, S. Piscitelli, T. Ricci, J. Morin, B. Angeletti, L. Mocochain and F. Sortino (2006). Hydrogeological insights at Stromboli volcano (Italy) from geoelectrical, temperature, and CO<sub>2</sub> soil degassing investigations, *Geophys. Res. Lett.*, 33, L17304.
- Finizola, A., J.F. Lénat, O. Macedo, D. Ramos, J.C. Thouret and F. Sortino (2004). Fluid circulation and structural discontinuities inside Misti volcano (Perù) inferred from self-potential measurements, *J. Volcanol. Geotherm. Res.*, 135, (4), 343–360.
- Fischer, T., J. Horálek, P. Hrubcová, V. Vavryčuk, K. Bräuer and H. Kämpfd (2014). Intra-continental earthquake swarms in West-Bohemia and Vogtland: A review, *Tectonophysics*, 611, 1–27. <https://doi.org/10.1016/j.tecto.2013.11.001>.
- Fischer, T.P. (2008). Fluxes of volatiles (H<sub>2</sub>O, CO<sub>2</sub>, N<sub>2</sub>, Cl, F) from arc volcanoes, *Geochem. J.*, 42, 21–38.
- Fisher, Q.J. and R.J. Nipe (1998). Fault sealing processes in siliciclastic sediments, in Jones, G., et al., eds., *Faulting and fault sealing in hydrocarbon reservoirs: Geological Society [London] Special Publication 147*, 117–134.
- Foley, S.F. and T.P. Fischer (2017). An essential role for continental rifts and lithosphere in the deep carbon cycle, *Nat. Geosc.*, 10, (12), 897–902. <https://doi.org/10.1038/s41561-017-0002-7>
- Forster, C.B., and J.P. Evans (1991). Fluid flow in thrust faults and crystalline thrust sheets, Results of combined field and modeling studies, *Geophys. Res. Lett.*, 18, 979–982.
- Fossen, H. and A. Rotevatn (2016). Fault linkage and relay structures in extensional settings—a review, *Earth Sci.*

- Rev., 154, 14-28.
- Fridriksson, T., B.R. Kristjánsson, H. Ármannsson, E. Margrétardóttir, S. Ólafsdóttir and G. Chiodini (2006). CO<sub>2</sub> emissions and heat flow through soil, fumaroles, and steam heated mud pools at the Reykjanes geothermal area, SW Iceland, *Appl. Geochem.*, 21, 1551-1569. <https://doi.org/10.1016/j.apgeochem.2006.04.006>.
- Fron dini, F., G. Chiodini, S. Caliro, C. Cardellini, D. Granieri, and G. Ventura (2004). Diffuse CO<sub>2</sub> degassing at Vesuvio, Italy, *Bull. Volc.*, 6, 642-651.
- Granieri, D., G. Chiodini, R. Avino and S. Caliro (2014). Carbon dioxide emission and heat release estimation for Pantelleria Island (Sicily, Italy), *J. Volc. Geother. Res.*, 275, 22-33, <https://doi.org/10.1016/j.jvolgeores.2014.02.011>.
- Granieri, D., R. Avino and G. Chiodini (2010). Carbon dioxide diffuse emission from the soil: ten years of observations at Vesuvio and Campi Flegrei (Pozzuoli), and linkages with volcanic activity, *Bull. Volc.*, 72, 103-118.
- Granieri, D., M.L. Carapezza, G. Chiodini, R. Avino, S. Caliro, M. Ranaldi, T. Ricci and L. Tarchini (2006). Correlated increase in CO<sub>2</sub> fumarolic content and diffuse emission from La Fossa crater (Vulcano, Italy): Evidence of volcanic unrest or increasing gas release from a stationary deep magma body?, *Geophys. Res. Lett.*, 33, L13316.
- Gurrieri, S. and M. Valenza (1988). Gas transport in natural porous mediums: a method for measuring CO<sub>2</sub> flows from the ground in volcanic and geothermal areas, *Rend. Soc. It. Min. Petrog.*, 43, 1151-1158.
- Hernández, P.A., G. Padilla, J. Barrancos, G. Melián, E. Padrón, M. Asensio-Ramos, F. Rodríguez, N. Pérez, M. Alonso and D. Calvo (2017). Geochemical evidences of seismo-volcanic unrests at the NW rift zone of Tenerife, Canary Islands, inferred from diffuse CO<sub>2</sub> emission, *Bull. Volcanol.*, 79, 30.
- Hutchison, W., T.A. Mather, D.M. Pyle, J. Biggs and G. Yirgu (2015). Structural controls on fluid pathways in an active rift system: A case study of the Aluto volcanic complex, *Geosphere*, 11, (3), 542-562.
- Jung, N.H., W.S. Han, Z.T. Watson, J.P. Graham and K.Y. Kim (2014). Fault-controlled CO<sub>2</sub> leakage from natural reservoirs in the Colorado Plateau, East-Central Utah, *Earth Planetary Sci. Lett.*, 403, 358-367.
- Kennedy, B.M., Y.K. Kharaka, W.C. Evans, A. Ellwood, D.J. DePaolo, J. Thordsen, G. Ambats and R.H. Mariner (1997). Mantle fluids in the San Andreas fault system, California, *Science*, 278, 1278-1281, <https://doi.org/10.1126/science.278.5341.1278>.
- Knipe, R.J., G. Jones and Q.J. Fisher (1998). Faulting, fault sealing and fluid flow in hydrocarbon reservoirs: an introduction, Geological Society, London, Special Publications, 147, vii-xx, <http://dx.doi.org/10.1144/GSL.SP.1998.147.01.01>.
- Lavecchia, G., F. Ferrarini, R. de Nardis, F. Visini and S. Barbano (2007). Active thrusting as a possible seismogenic source in Sicily (Southern Italy): some insights from integrated structural-kinematic and seismological data, *Tectonophysics*, 445, 145-167.
- Lee, H., J.D. Muirhead, T.P. Fischer, C. J. Ebinger, S.A. Kattenhorn, Z.D. Sharp and G. Kianji (2016). Massive and prolonged deep carbon emissions associated with continental rifting, *Nature Geosci.*, 9, 145-149.
- Lewicki, J.L., W.C. Evans, G.E. Hilley, M.L. Sorey, J.D. Rogie and S.L. Brantley (2003). Shallow soil CO<sub>2</sub> flow along the San Andreas and Calaveras Faults, California, *J. Geophys. Res.*, 108, B4, 2187.
- Mailloux, B.J., M. Person, S. Kelley, N. Dunbar, S. Cather, L. Strayer and P. Hudleston (1999). Tectonic controls on the hydrogeology of the Rio Grande rift, New Mexico, *Water Resour. Res.*, 35, 2641-2659, <https://doi.org/10.1029/1999WR900110>.
- Monaco, C., S. Mazzoli and L. Tortorici (1996). Active thrust tectonics in western Sicily (southern Italy): the 1968 Belice earthquakes sequence, *Terra Nova*, 8, 372-381.
- Morelli, A. and S. Pondrelli (1998). Il terremoto del Belice del 1968. In: Poster presented at Conference "Trenta anni di terremoti in Italia: dal Belice a Colfiorito", Erice, Sicily, 14-18 July.
- Mörner, N.A. and G. Etiope (2002). Carbon degassing from the lithosphere, *Global and Planetary Change*, 33, 185-203.
- Ni, Y., F. Liao, J. Dai, C. Zou, X. Wu, D. Zhang, S. Huang, R. Chen and T. Wang (2014). Studies on gas origin and gas source correlation using stable carbon isotopes – A case study of the giant gas fields in the Sichuan Basin, China, *En. Explor. Exploit.*, 32, 1 41-74.
- O'Leary M.H. (1988). Carbon isotopes in photosynthesis, *Bioscience*, 38, 328-336.
- Oertel, C., J. Matschullat, K. Zurba, F. Zimmermann and S. Erasmí (2016). Greenhouse gas emissions from soils-A review, *Chem. Erde-Geochem.* 76, 3, 327-352.
- Padilla, G.D., P.A. Hernández, N.M. Pérez, E. Pereda, E. Padrón, G. Melián, J. Barrancos, F. Rodríguez, S. Dionis, D. Calvo, M. Herrera, W. Strauch and A. Muñoz (2014). Anomalous diffuse CO<sub>2</sub> emissions at the Masaya Volcano

- (Nicaragua) related to seismic-volcanic unrest, *Pure Appl. Geophys.*, 171, 1–14.
- Padrón, E., P.A. Hernández, T. Toulkeridis, N.M. Pérez, R. Marrero, G. Melián, G. Virgili and K. Notsu (2008). Diffuse CO<sub>2</sub> emission rate from Pululahua and the lake-filled Cuicocha calderas, Ecuador, *J. Volcanol. Geoth. Res.*, 176, 163-169
- Raich, J.W. and A. Tufekciogul (2000). Vegetation and soil respiration: Correlations and controls, *Biogeochem.*, 48, 71-90.
- Raich, J.W. and C.S. Potter (1995). Global patterns of carbon dioxide emissions from soils, *Global Biogeochem.*, Cy. 9, 1, 23-36.
- Raich, J.W. and W.H. Schlesinger (1992), The global carbon dioxide flux in soil respiration and its relationship to vegetation and climate, *Tellus*, 44B, 81–99.
- Rastogi, M., S. Singh and H. Pathak (2002). Emission of carbon dioxide from soil, *Curr. Sci. India*, 82, 5, 510-517.
- Rawling, G.C., L.B. Goodwin and J.L. Wilson (2001). Internal architecture, permeability structure, and hydrologic significance of contrasting fault-zone types, *Geology*, 27, 43-46.
- Rowland, J.V. and S.F. Simmons (2012). Hydrologic, magmatic, and tectonic controls on hydrothermal flow, Taupo volcanic zone, New Zealand: implications for the formation of epithermal vein deposits, *Econ. Geol.*, 107, 427-457.
- Rowland, J.V. and R.H. Sibson (2004). Structural controls on hydrothermal flow in a segmented rift system, Taupo Volcanic Zone, New Zealand, *Geofluids*, 4, 259–283.
- Saffer, D.M. (2015). The permeability of active subduction plate boundary faults, *Geofluids*, 15, (1–2), 193-215. <https://doi.org/10.1002/9781119166573.ch18>.
- Savini, A., E. Malinverno, G. Etiope, C. Tessarolo and C. Corselli (2009). Shallow seep-related seafloor features along the Malta plateau (Sicily channel - Mediterranean Sea): morphologies and geo-environmental control of their distribution, *Mar. Petrol. Geol.*, 26, (9), 1831-1848, <https://doi.org/10.1016/j.marpetgeo.2009.04.003>.
- Scholz, C.H. and M.H. Anders (1994). The permeability of faults, *Proceedings of Workshop LXIII, The Mechanical Involvement of Fluids in Faulting*, U.S. Geol. Surv. Open File Rep., 94-228, 247-253.
- Sgroi, T., R. De Nardis and G. Lavecchia (2012). Crustal structure and seismotectonics of central Sicily (southern Italy): new constraints from instrumental seismicity, *Geophys. J. Int.*, 189, 1237-1252.
- Shinohara, H. (2013). Volatile flux from subduction zone volcanoes: insights from a detailed evaluation of the fluxes from volcanoes in Japan, *J. Volcanol. Geotherm. Res.*, 268, 46-63.
- Sibson, R.H. (1977). Kinetic shear resistance, fluid pressures and radiation efficiency during seismic faulting, *Pure Appl. Geophys.*, 115, 387-400.
- Sibson, R.H. and J.V. Rowland, (2003). Stress, fluid-pressure, and structural permeability in seismogenic crust, North Island, New Zealand, *Geophys. J. Int.*, 154, 584-594.
- Sinclair, A.J. (1974). Selection of thresholds in geochemical data using probability graphs, *J. Geochem. Explor.*, 3, 129–149.
- Skelton, A., M. Andrén, H. Kristmannsdóttir, G. Stockmann, C.M. Mörth, Á. Sveinbjörnsdóttir, S. Jónsson, E. Sturkell, H.R. Guðrúnardóttir, H. Hjartarson, H. Siegmund and I. Kockum (2014). Changes in groundwater chemistry before two consecutive earthquakes in Iceland, *Nat. Geosci.*, 7, 752–756.
- Swan, A.R.H. and M. Sandilands (1995). *Introduction to Geological Data Analysis*, Blackwell Science, Oxford, UK.
- Tarchini, L., M. Ranaldi, M.L. Carapezza, M.G. Di Giuseppe, R. Isaia, C. Lucchetti, E. P. Prinzi, F. D’Assisi Tramparulo, A. Trioano and S. Vitale (2018). Multidisciplinary studies of diffuse soil CO<sub>2</sub> flux, gas permeability, self-potential, soil temperature highlight the structural architecture of Fondi di Baia craters (Campi Flegrei caldera, Italy), *Ann. Geophys.*, 61, 12.
- Taylor, B.E. (1986). Magmatic volatiles: isotopic variation of C, H and S, *Rev. Mineral.*, 16, 185–225.
- Visini, F., R. De Nardis and G. Lavecchia (2010). Rates of active compressional deformation in central Italy and Sicily: evaluation of the seismic budget, *Int. J. Earth Sci.*, 99, 243-264.
- Viveiros, F., M. Marcos, C. Faria, J.L. Gaspar, T. Ferreira and C. Silva (2017). Soil CO<sub>2</sub> Degassing Path along Volcano-Tectonic Structures in the Pico-Faial-São Jorge Islands (Azores Archipelago, Portugal), *Front. Earth Sci.*, 5, 50.
- Wang, C.Y. and M. Manga (2010). Hydrologic responses to earthquakes and a general metric, *Geofluids*, 10, 206–16.
- Weinlich, F.H., V. Stejskal, M. Teschner, and J. Poggenburg (2013). Geodynamic processes in the NW Bohemian swarm earthquake region, Czech Republic, identified by continuous gas monitoring, *Geofluids*, 13, 305–330.
- Werner, C., Bergfeld, D., Farrar, C. Doukas, M. P., Kelly, P. J., and C. Kern (2014). Decadal-scale variability of diffuse

- CO<sub>2</sub> emissions and seismicity revealed from long-term monitoring (1995-2013) at Mammoth Mountain, California, USA, *J. Volcanol. Geotherm. Res.*, 289, 51-63.
- Werner, C., T. Hurst, B. Scott, S. Sherburn, B.W. Christenson, K. Britten, J. Cole-Baker and B. Mullan (2008). Variability of passive gas emissions, seismicity, and deformation during crater lake growth at White Island Volcano, New Zealand, 2002–2006, *J. Geophys. Res.*, 113, B01204.
- Werner, C. and C. Cardellini, (2006). Comparison of carbon dioxide emissions with fluid upflow, chemistry, and geologic structures at the Rotorua geothermal system, New Zealand. *Geothermics* 35, 221–238, <http://dx.doi.org/10.1016/j.geothermics.2006.02.006>.
- Whiticar, M.J. (1994). Correlation of natural gases with their source. In Magoon, L.B., and Dow, W.G. (Eds), *The Petroleum System—From Source to Trap*. AAPG Mem., 60, 261– 283.
- Wycherley, H., A. Fleet and H. Shaw (1999). Some observations on the origins of large volumes of carbon dioxide accumulations in sedimentary basins, *Mar. Petrol. Geol.*, 16, 489–94.
- Yehya, A., Z. Yang, and J.R. Rice (2018). Effect of fault architecture and permeability evolution on response to fluid injection, *J. Geophys. Res. - Solid Earth*, 123, 9982-9997.
- Zhang, M., Z. Guo, Y. Sano, L. Zhang, Y. Sun, Z. Cheng and T.F. Yang (2016). Magma-derived CO<sub>2</sub> emissions in the Tengchong volcanic field, SE Tibet: implications for deep carbon cycle at intra-continent subduction zone, *J. Asian Earth Sci.*, 127, 76-90.

**\*CORRESPONDING AUTHOR: Sofia DE GREGORIO,**

Istituto Nazionale di Geofisica e Vulcanologia,

sezione di Palermo – Via Ugo La Malfa, 153

90146 - Palermo Italy;

e-mail: [sofia.degregorio@ingv.it](mailto:sofia.degregorio@ingv.it)

© 2020 the Istituto Nazionale di Geofisica e Vulcanologia.

All rights reserved